LETTERS
https://doi.org/10.1038/s41550-018-0574-1

nature astronomy

Corrected: Author correction

Cryovolcanic rates on Ceres revealed by topography

Michael M. Sori[1*], Hanna G. Sizemore[2], Shane Byrne[1], Ali M. Bramson[1], Michael T. Bland[3], Nathaniel T. Stein[4] and Christopher T. Russell[5]

Cryovolcanism, defined here as the extrusion of icy material from depth, may be an important planetary phenomenon in shaping the surfaces of many worlds in the outer Solar System and revealing their thermal histories[1–3]. However, the physics, chemistry and ubiquity of this geologic process remain poorly understood, especially in comparison to the better-studied silicate volcanism on the terrestrial planets. Ceres is the only plausibly cryovolcanic world to be orbited by a spacecraft up to now, making it the best opportunity to test the importance of cryovolcanism on bodies in the outer Solar System and compare its effects to silicate volcanism on terrestrial planets. Here, we analyse images from NASA's Dawn mission[4] and use the finite element method to show that Ceres has experienced cryovolcanism throughout its geologic history, with an average cryomagma extrusion rate of ~10^4 m^3 yr^{-1}. This result shows that volcanic phenomena are important on Ceres, but orders of magnitude less so than on the terrestrial planets.

The prominent mountain Ahuna Mons on Ceres (Fig. 1) has been interpreted as a cryovolcanic construct[5]. Ahuna Mons has an upper age limit of 240 million years (Myr) derived from crater size–frequency analysis of units that it superposes[5], but it may be much younger because the mountain itself is too small and has too few craters to be reliably dated. An outstanding problem in the analysis of Ahuna Mons has been why only one prominent cryovolcano was observed, as the general trend of planetary cooling makes it difficult to construct a thermal history that would allow for cryovolcanism in the past hundreds of million years[5], but not earlier. A proposed solution is that cryovolcanic domes viscously relax over geologic timescales, precluding constructs older than Ahuna Mons from easy identification[6]. This process would require domes to have a softer rheology than the crust of Ceres as a whole, which on average experiences only modest viscous relaxation[7,8]. This hypothesis has been shown to be physically plausible on the basis of numerical models[6] but has not been tested observationally. Here we identify viscously relaxed domes using a combination of topographic analysis and flow modelling, allowing for a reconstruction of Ceres's cryovolcanic history.

We analysed images from the Dawn Framing Camera images to search for large domes that may be old cryovolcanic constructs. We identified 32 such domes, which are all >10 km in diameter. Small mounds at the kilometre scale or smaller also exist but are likely to have an impact-related origin[9]. We studied the heights and morphologies of the domes using topography that has been produced from Framing Camera stereo imagery[10]. The 32 domes have surface relief >1 km, and have convex-up morphology. We excluded 10 of the 32 domes from further analysis on the basis of an inability to reliably measure their physical dimensions with sufficient precision. In some of these cases, most of the original dome's topography appears to have been destroyed by a large impact crater, and in other cases, the dome is surrounded by several large craters in a location where impact ejecta may be expected to accumulate. Our conservative selection of 22 domes (which includes Ahuna Mons) increases the likelihood that we are correctly identifying cryovolcanic constructs but may imply that we are preferentially selecting younger domes. Some of these domes have previously been identified[11] as 'tholi', but we use the more general term 'domes' to encompass both tholi and montes. Tholi on other planets have often been identified as volcanic in origin (see, for example, ref. [12]).

Of the 22 domes selected for further analysis (Fig. 1a), we measured their average diameters and heights, and calculated an aspect ratio (defined herein as the ratio of surface relief to average basal diameter) of each dome. We additionally searched Framing Camera images for any anomalously bright features on the domes, which are observed at Ahuna Mons[13]. We calculated average diameters ranging from 16 to 86 km, surface relief ranging from 1.1 to 4.4 km, and volumes of order 10^2–10^3 km^3 (see Methods). An example of one of the 22 domes studied is shown in the middle panel of Fig. 1b. This dome, located in Begbalel crater, contains a similar volume to Ahuna Mons, but with greater diameter, less topographic relief and lower slopes. Data for all analysed domes can be found in Supplementary Tables 1 and 2.

The viscous relaxation hypothesis predicts that domes flatten over time, conserving volume but increasing in diameter and decreasing in surface relief. However, cryovolcanic episodes may involve variable volumes of cryomagma, cautioning against directly comparing surface relief of domes as a test of viscous relaxation. Instead, we argue that dome aspect ratio is the more appropriate parameter to consider. The slopes and aspect ratio of Ahuna Mons seem to be controlled by the angle of repose[5], and we assume that those values represent the initial conditions of other putative cryovolcanic domes. The aspect ratios of the 22 studied domes are shown in Fig. 2a as a function of latitude. They are statistically different from a uniform distribution of aspect ratios across all latitudes (see Methods).

We tested the viscous relaxation hypothesis using finite element method (FEM) numerical models that solve the Stokes equations (see Methods). The rheological equation that we used is based on laboratory work that considers dislocation creep and grain boundary sliding of ice[14] and the effects of silicate or salt contamination[15]. The temperature inputs to the FEM flow model are calculated with a

[1]Lunar and Planetary Laboratory, University of Arizona, Tucson, AZ, USA. [2]Planetary Science Institute, Tucson, AZ, USA. [3]USGS Astrogeology Science Center, Flagstaff, AZ, USA. [4]Division of Geological and Planetary Sciences, California Institute of Technology, Pasadena, CA, USA. [5]Earth, Planetary, and Space Sciences, UCLA, Los Angeles, CA, USA. *e-mail: michael.sori@gmail.com

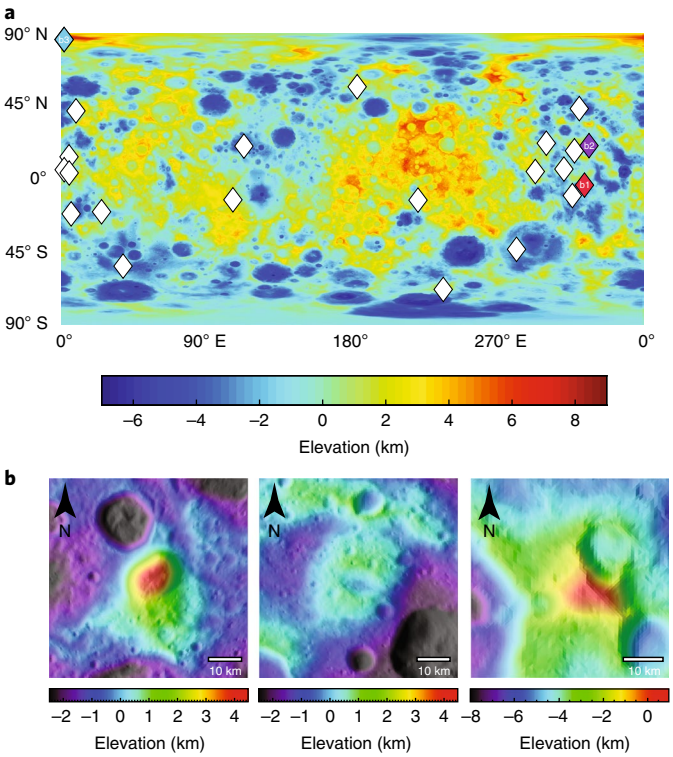

Fig. 1 | Observations of domes on Ceres. a, Locations of the large domes analysed here, overlying a topographic map of Ceres in cylindrical projection. **b**, Left: elevation overlying shaded topographic relief of Ahuna Mons, a putative cryovolcanic construct (red diamond in **a**). Middle: one of the other 21 domes analysed here, located in Begbalel crater (violet diamond in **a**). Right: Yamor Mons, one of the other 21 domes analysed here, located near the north pole (light blue diamond in **a**).

semi-implicit thermal model[16] that balances insolation with subsurface conduction and considers latitude, surface slope and the orbital changes of Ceres. We initialize the flow model with a cryovolcano in the shape of Ahuna Mons and assume that it is emplaced instantaneously at a point in the past. The flow model calculates the viscous deformation to the present day of a cryovolcano at every 5° latitude. Although it is possible that not every putative cryovolcano was emplaced with the same shape as Ahuna Mons, the resulting distribution of aspect ratios should be diagnostic provided that Ahuna Mons is not an outlier in initial shape. Results of predicted aspect ratios are plotted with the observations of aspect ratios for the 22 domes in Fig. 2a, for the case in which the domes are assumed to be 50% ice by volume. Aspect ratios vary with latitude because of the strong dependence of viscosity on temperature.

Constraints on age and composition come from an independent combination of geophysical observations and consideration of faculae (anomalously bright areas). Sodium carbonates are present on the flanks of Ahuna Mons and are consistent with a cryovolcanic origin[13,17]. Models of impact-induced lateral mixing show that faculae are expected to have an average lifetime of ~300 Myr before they are buried or destroyed by new impacts[13]. We did not observe faculae on any of the non-Ahuna domes. If those domes once hosted faculae, they are likely to be older than ~100 Myr (a conservative estimate based on the lateral extent of impact ejecta, a free parameter in the mixing model) in order for those faculae to have disappeared. Our FEM flow models imply that the domes thus have a maximum volumetric ice content of 70%; if the domes had more ice, they would have relaxed more quickly than faculae disappear. Some faculae do exist in flat terrain on Ceres but are associated with impact craters, not relaxed dome topography[13]. For the domes to viscously relax at all, they must have average ice content greater than typical Cerean crust, which is relatively immobile at these spatial scales[7,8]. Such an ice enhancement may be expected if Cerean cryomagma is formed by partial melting, rather than complete melting, of portions of the interior. A maximum ice content[7] of the shallow subsurface of Ceres is 30–40%, implying that the domes are 30–70% ice by volume. Our nominal results are thus presented assuming an ice volume of 50%. The non-icy component is probably a combination of rocks, salts and clathrates[8]. Some heterogeneity in cryomagma composition may exist, which could explain some deviation in the observations from the modelled lines in Fig. 2a.

A general good agreement between model predictions and observations in Fig. 2a supports the viscous relaxation hypothesis, and there are several specific observations that may be diagnostic. The polar dome Yamor Mons[18] (the only feature at latitude >70°) has the largest aspect ratio of any of the domes, and this is the same as the aspect ratio of Ahuna Mons within uncertainty. This property is expected because the poles of Ceres are too cold (<100 K annual-average temperature, compared with ~155 K at the equator) to allow ice to flow at any geologic timescales. There exist no high-latitude domes with lower aspect ratios than Ahuna Mons, including the ten domes excluded from analysis. The presence of such a dome would complicate the viscous relaxation hypothesis for the reason mentioned above. There exist no low-latitude domes with high aspect ratios, other than geologically young Ahuna Mons. The presence of such a dome would also be at odds with the viscous relaxation hypothesis because if such a feature was old, it should have experienced extensive deformation. Finally, mid-latitude domes display a wider range of aspect ratios than low-latitude domes. This property is expected because aspect ratios of cooler mid-latitude domes should be more sensitive to their age. No individual property listed above proves a cryovolcanic origin, but collectively they are highly suggestive of viscous relaxation of relatively ice-rich topography.

Alternative hypotheses do not fully explain the observations, in particular the young age of Ahuna Mons. Diapirism driven by differential topographic loading may plausibly cause doming on Ceres[19], but does not reproduce the high-relief, high-aspect-ratio of Ahuna Mons under realistic physical parameters and should not result in the latitudinal trends that we observed because it predicts that dome topography would be composed of the relatively strong average Cerean crust. Diffusion caused by meteoritic bombardment may be important for the evolution of topography at the kilometre scale or less, but it is unlikely to be the dominant modification mechanism of features tens of kilometres or greater in scale[20,21]. The results here do not imply that diapirs or topographic diffusion are absent or negligible on Ceres, only that they are unlikely to fully explain the shape and size of its observed domes.

We can invert the observations to constrain the cryovolcanic history of Ceres, which requires estimates of volume and age for each dome. We measure the volume of each from our topographic analysis (see Methods). Our models constrain the age of each dome by estimating the time that it takes for a dome with the aspect ratio of Ahuna Mons to relax into that dome's present observed aspect ratio. We estimate the age of each dome assuming a nominal ice content of 50%, finding the observed domes to be 100s of million years old (Fig. 2b). Older domes are likely to be unidentifiable, with the exception of the high-latitude example, Yamor Mons. Yamor Mons has an unconstrained age from our models because it is neither predicted nor observed to relax viscously. Crater size–frequency analysis is not reliable on the domes themselves because of their small size, but our results are consistent with the age constraints that exist in underlying terrain. For example, the unnamed dome in Fig. 1b (middle panel) is located in a crater that is estimated to have an age[22] of 1.9 billion years (Gyr). Thus, 1.9 Gyr is an upper limit for the age of the dome, which we estimate from our models to have

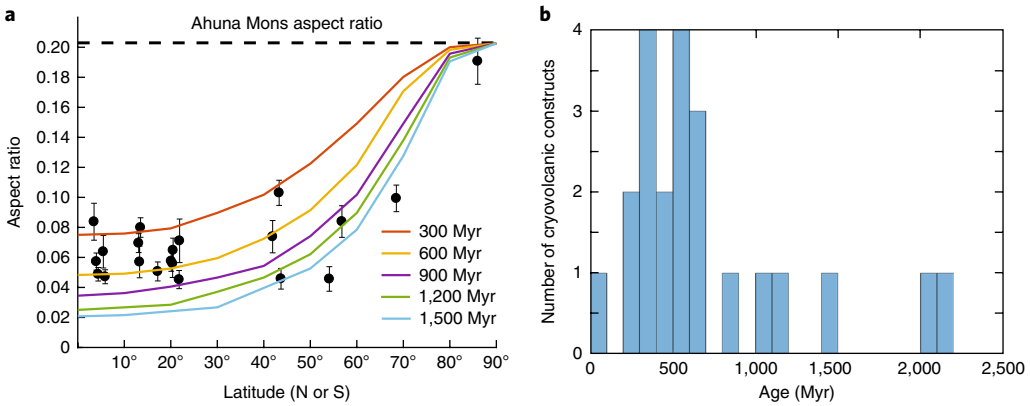

Fig. 2 | Model results of dome evolution and ages. a, Aspect ratios of 21 domes on Ceres (black dots), compared with the aspect ratio of Ahuna Mons (dashed line) and the modelled aspect ratios of viscously deformed cryovolcanoes at various times after formation (solid lines). Error bars represent uncertainty in observations of aspect ratios as defined in the Methods. **b**, Histogram of ages inferred by our FEM models for the 22 observed domes plotted in **a**. Ahuna Mons is assumed to have an age of zero relative to the other domes and is represented by the leftmost bar. The polar dome Yamor Mons has an unconstrained age from our viscous relaxation model because it is too cold to deform over any geologic timescales; it is plotted in Fig. 2b with an age of 1 Gyr to be consistent with geologic mapping constraints[18]

an age of 510 Myr. All of these ages assume an initial condition with the aspect ratio of Ahuna Mons, and thus the age of Ahuna Mons should be added to the results. Because Ahuna Mons is young, our conclusions are robust to this uncertainty.

Our results are consistent with a cryovolcanic construct forming, on average, every ~50 Myr over the past ~1 Gyr with an effusion rate of order 10^4 $m^3 yr^{-1}$. Because of model uncertainties and the possibility that not all domes are cryovolcanic, we report only an order of magnitude estimate, and we use statistical tests to determine whether these cryovolcanic eruptions are uniform in time and space (see Methods). Over the past 1 Gyr, the distribution of cryovolcanism as a function of time is not statistically distinguishable from a constant distribution in which a cryovolcano forms every 50 Myr; we cannot confidently identify an increase or decrease in activity. Spatially, our tests reveal that eruptions are not uniformly distributed over Ceres, implying lateral heterogeneity of cryovolcanism. Some domes may be clustered in the site of an ancient impact basin[23], possibly suggesting a genetic link. Domes do not show trends with crustal thickness, suggestive that magmatic activity may initiate in Ceres's crust and not beneath.

Cryovolcanic features other than the large domes analysed here may exist on Ceres. In particular, faculae associated with impact craters have been identified and probably represent endogenic or impact-triggered activity involving upwelling of liquids[24–26]. If the faculae are cryovolcanic, they may represent a non-negligible contribution to Ceres's recent cryovolcanic history, depending on their thickness. However, topographic constraints imply that most of the faculae are likely to be only metres thick[27] outside the central dome at Occator crater, implying that the bulk volume of cryovolcanic activity is dominated by the large domes unless many more faculae, in addition to those observed, formed in the past few million years. Intrusions, which have been proposed to be important for lava dome growth on the Earth[28], may also be possible, and can be quantified if high-resolution gravity data or additional geophysical constraints are ever acquired for Ceres, as has been done for the Moon[29].

Our estimated average cryovolcanic rates of 10^4 $m^3 yr^{-1}$ for Ceres can be compared with rates of basaltic volcanism on terrestrial planets to assess the relative importance of the two processes across different bodies. The volcanic eruption rates on Earth[30] and Venus[31] are of order 10^9 $m^3 yr^{-1}$ over the past few million years. The volcanic eruption rates for the Moon[32] and Mars[33] are of order 10^6 $m^3 yr^{-1}$ and 10^7 $m^3 yr^{-1}$, respectively, which apply to the past ~3.9 Gyr. The rates for the terrestrial objects are at least an order of magnitude greater than

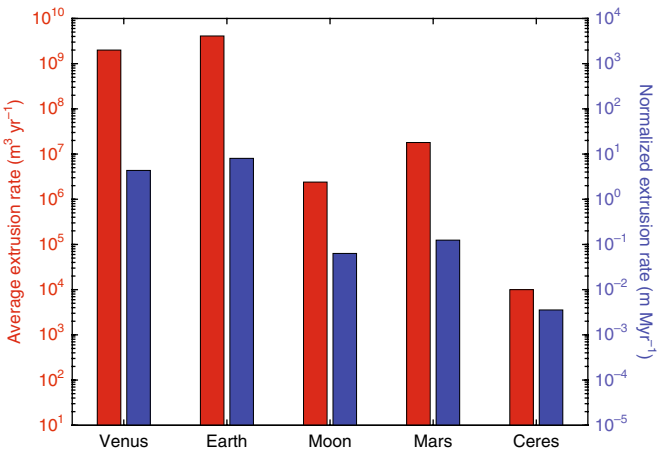

Fig. 3 | Comparison of volcanic rates with those of other planets. Average basaltic extrusion rates estimated for Venus[31], the Earth[30], the Moon[32] and Mars[33] compared with our inferred average cryovolcanic extrusion rate for Ceres. Results displayed both as volume per year (red) and as volume per year divided by surface area of the planet (blue).

the rates for Ceres even when normalized for surface area (Fig. 3). Therefore, although cryovolcanism is an important process in shaping the geomorphology of Ceres, it is not as important as basaltic volcanism is on the terrestrial planets.

Eruption rates on other cryovolcanic worlds are less constrained. One proposed resurfacing rate for Europa[34] would imply an eruption rate of 10^9 $m^3 yr^{-1}$ in the upper limit of all resurfacing being cryovolcanic. This upper limit is orders of magnitude higher than our estimate for Ceres, perhaps representing the important role of tidal heating on Europa. Whether similar conclusions hold true for other potentially cryovolcanic objects like Titan and Pluto can be tested as their geologic histories become better understood.

Methods

Measurements. We measure physical dimensions of domes using a topographic map of Ceres[10] constructed from stereo imagery. For each dome, eight topographic profiles were extracted through the centre of the dome. In the nominal case, these topographic profiles were extracted along uniform 22.5° increments (that is, a N–S profile, a NNE–SSW profile and so on). In practice, the direction of some topographic profiles was adjusted to avoid impact craters at the dome base, which would bias measurements. For each topographic profile, the distance between the

maximum elevation and the elevation at the base was called the height, and the distance between the base at either end of the topographic profile was called the diameter. The choice of where the 'base' of the dome occurs was made for each topographic profile. The base was considered the point where the profile reaches the approximate elevation of the surrounding terrain and experiences a break in slope. The slope break generally represents a change in concavity from the convex-up domes to the surrounding terrain, similar to methodology used to identify the base of some terrestrial volcanic edifices[35]. The identification of the base was checked with images, but performed with topography, where slope breaks were generally easily identifiable. Using topography as the primary dataset to identify the boundaries of volcanic features, although not completely objective, is generally less subjective than using other datasets[35] and has even allowed for automation in some terrestrial cases[36]. The dome height and dome diameter were interpreted as the average of the heights and diameters across all the topographic profiles, and the standard deviation of the heights and diameters across all the topographic profiles was interpreted as the uncertainty. The volume of each dome was calculated as $h'\pi(d/2)^2$, where d is the diameter of the dome and h' is the average height of the dome.

The effusion rate that we estimate is the sum of the volumes of all domes formed in the past 1 Gyr (according to our flow models) divided by 1 Gyr. For our nominal case of a composition of 50% ice by volume, this effusion rate is 24,000 $m^3 yr^{-1}$. Considering the entire range of possible ice contents of 30–70% would cause the resulting effusion rate to range from 21,000 to 34,000 $m^3 yr^{-1}$. These numbers may be upper limits if some of the domes that we measure are formed tectonically instead of cryovolcanically. The estimates for an individual dome may be a lower limit if some of the dome's volume is partially masked by flexure, but this effect has not been observed in previous spectral analysis[37] nor in our work here. If flexure was occurring, we calculate it to be a relatively minor effect: Ahuna Mons would cause a maximum deflection of an underlying 100-km-thick elastic plate by 70 m, assuming a Poisson's ratio of 0.25 and a Young's modulus of 10^{10} Pa. To respect all the uncertainties in composition, dome identification and flexural parameters, we report only an order of magnitude estimate of $10^4 m^3 yr^{-1}$.

Viscous flow model. Our FEM viscous flow model uses the software Elmer/Ice[38], an open-source code developed to address problems in terrestrial ice dynamics and which we have previously adapted for use in planetary contexts[6,39]. We use this software to solve the Stokes equations for conservation of mass and momentum, which are respectively:

$$\nabla \mathbf{u} = 0 \tag{1}$$

$$\nabla \sigma + \rho \mathbf{g} = 0 \tag{2}$$

$\mathbf{u}$ is the velocity vector, $\mathbf{g}$ is the gravity vector, $\boldsymbol{\sigma}$ is the Cauchy stress tensor and ρ is the material density.

We use a rheology that considers strain rates for two deformation mechanisms: dislocation creep and grain boundary sliding. The equations for strain rate for these two deformation mechanisms, are, respectively:

$$\dot{\varepsilon}_{\mathrm{dis}} = \frac{3^{2.5}}{2} 4{,}00{,}000 \mathrm{e}^{-8\phi - \frac{60{,}000}{RT}} \tau^4 \tag{3}$$

$$\dot{\varepsilon}_{\mathrm{GBS}} = \frac{3^{1.4}}{2} 0.0039 \mathrm{e}^{-3.6\phi - \frac{40{,}000}{RT}} \tau^{1.8} d^{-1.4} \tag{4}$$

τ is deviatoric stress in MPa, ϕ is non-ice volume fraction (in this case, the sum of silicates and salts), d is ice grain size in metres, R is the gas constant and T is temperature in K. For features of the size studied here, basal slip is limited by grain boundary sliding, and diffusion creep is negligible[6]. These equations are only applicable for temperatures <250 K, which we find appropriate for Ceres according to our thermal model.

Given the likely multi-compositional nature of Ceres's crust, the effects of the non-ice component on deformation are particularly important. The above equations treat the non-ice component as being relatively undeformable inclusions compared with the ice. Thus, the non-ice components effectively act as obstacles impeding flow, which is quantified using an exponential law that was determined experimentally[15]. This behaviour applies to silicates[15,40] and salts[41,42] up to a minimum ice content determined by the packing density of the material, below which viscosity increases substantially[15].

Boundary conditions in our flow model are that the top surface is a free surface, and that no sliding occurs at the bottom surface. The FEM domain is meshed with nodes every 100 m, and we find that flow velocities do not change significantly by increasing node density.

The model assumes that uplift is absent or negligible compared with viscous flow. Although uplift could conceivably occur if a cryomagma chamber freezes, owing to the density difference between liquid water and solid ice, it is only important under a narrow set of circumstances: the chamber must be full or near-full when it freezes, the chamber must be tens of kilometres greater in diameter, and volume expansion must not be accommodated by closure of porosity (which is likely to be created by impacts on airless bodies[43,44]). Freezing of individual subsurface melt pockets may occur, but suffer from similar caveats as above. Furthermore, our model begins with the present topography of Ahuna Mons as a starting point, so uplift would only be relevant for other domes in our model if it has not yet ceased at Ahuna Mons.

Thermal model. Temperature inputs into the viscous flow models are calculated with a one-dimensional semi-implicit thermal model[16]. The model simulates energy balance at the surface from solar insolation, blackbody radiation, and thermal conduction through subsurface numerical layers. It also includes reradiation from surrounding flat terrain back towards the sloped dome surface. At the boundaries of each of subsurface layers, we solve the thermal diffusion equation:

$$\rho c \frac{\partial T}{\partial t} = \frac{\partial}{\partial z}\left(k \frac{\partial T}{\partial z}\right) \tag{5}$$

ρ is the material density, c is heat capacity, T is temperature, t is time, z is depth and k is thermal conductivity. The equation solved at the surface is:

$$E\varphi T_s^4 = S(1-A)\cos(i) + k\frac{\partial T}{\partial z} \tag{6}$$

E is the emissivity (assumed to be 0.9), φ is the Stefan–Boltzmann constant, T_s is the temperature at the surface, S is the solar flux at Ceres, A is the surface albedo and i is the incidence angle of sunlight, which also accounts for surface slope. The surface albedo is assumed to be 0.1, and we impose a small geothermal heat flux[45] of 1 mW m^{-2}. Annual-average temperatures for each feature are calculated according to its latitude, evolving surface slope, and time-dependent obliquity, eccentricity and semi-major axis[46] by calculating temperature every 500 s throughout a Cerean year.

Statistical tests. We use a Kolmogorov–Smirnov statistical test to determine whether the distribution of aspect ratios of observed domes as a function of latitude could be distinguished from the null hypothesis in which aspect ratios are uniform with latitude. We found that this null hypothesis could be rejected at a high significance level (<1%), implying that dome aspect ratios do vary as a function of latitude.

We also use a Kolmogorov–Smirnov statistical test to determine whether the cryovolcanic history that we infer is statistically different from a rate in which a cryovolcano is formed anywhere on the surface of Ceres in regular time intervals. We perform this test only for the past billion years of Cerean history, because there is likely to be a systematic bias in that structures older than 1 Gyr are more likely to be unidentified because of modification from viscous relaxation or other processes. We find that our inferred distribution of cryovolcanic constructs as a function of time (Fig. 2b) is not statistically different at a 10% significance level from a constant distribution in which a cryovolcano has formed every 50 Myr over the past 1 Gyr. Therefore, we cannot identify with confidence an increase or decrease in cryovolcanic activity in the past 1 Gyr.

We use a Monte Carlo procedure to determine whether the spatial distribution of domes is likely to represent a uniform distribution over the surface of Ceres. We assume that cryovolcanic activity began 1 Gyr ago, and we create a dome with the size and shape of Ahuna Mons at a random latitude and longitude on Ceres's surface every 50 Myr. The longitude is sampled from a uniform distribution between 0° and 360°, while the latitude is sampled with the equation

$$\theta = -90^{\circ} + \arccos(2x-1) \tag{7}$$

where x is chosen from a uniform distribution between 0 and 1. Based on our observations, we assume that a dome effectively becomes undetectable when it deforms into a feature with an aspect ratio of 0.03 or less (Fig. 2a); for example, we expect this limit to be reached for Ahuna Mons after 700 Myr based on our FEM models. We calculate the percentage of domes expected to remain recognizable in the present day at a latitude of 30° or less. This procedure is repeated 10,000 times. The observed percentage of domes from Dawn topography that are at these low latitudes is 68%. The percentage of the 10,000 modelled cases with 68% or more low-latitude domes recognizable in the present day is only 2%. This percentage decreases if we assume that cryovolcanism on Ceres was initiated earlier than a biollion years ago. Therefore, we conclude the locations of observed domes on Ceres are unlikely to be sampled from a uniform distribution.

Finally, we used a derived map of crustal thickness on Ceres[37] to determine whether the 21 domes and Ahuna Mons preferentially occur in regions of thin crust. The average crustal thickness at the 22 domes is 42.2 km, compared with the average value[37] for Ceres as a whole of $41.0^{+3.2}_{-4.7}$ km. The absolute thickness values are dependent on some model parameters considered in the derivation of the crustal thickness map, but they are accurate in a relative sense. Domes are not preferentially located in regions of unusually thin or thick crust.

Data availability

The data that support the plots within this paper and other findings of this study are available from the corresponding author upon reasonable request. The data come from NASA's Dawn mission and are also publically available in the NASA Planetary Data System (https://pds.nasa.gov).

Received: 10 April 2018; Accepted: 13 August 2018;
Published online: 17 September 2018

References

1. Kargel, J. S. Brine volcanism and the interior structures of asteroids and icy satellites. *Icarus* **94**, 368–390 (1991).
2. Schenk, P. M., McKinnon, W. B., Gwynn, D. & Moore, J. M. Flooding of Ganymede's bright terrains by low-viscosity water-ice lavas. *Nature* **410**, 57–60 (2001).
3. Quick, L. C., Glaze, L. S. & Baloga, S. M. Cryovolcanic emplacement of domes on Europa. *Icarus* **284**, 477–499 (2017).
4. Russell, C. T. et al. Dawn arrives at Ceres: exploration of a small, volatile-rich world. *Science* **353**, 1008–1010 (2016).
5. Ruesch, O. et al. Cryovolcanism on Ceres. *Science* **353**, aaf4286 (2016).
6. Sori, M. M. et al. The vanishing cryovolcanoes of Ceres. *Geophys. Res. Lett.* **44**, 1243–1250 (2017).
7. Bland, M. T. et al. Composition and structure of the shallow subsurface of Ceres revealed by crater morphology. *Nature Geosci.* **9**, 528–542 (2016).
8. Fu, R. R. et al. The interior structure of Ceres as revealed by surface topography. *Earth. Planet. Sci. Lett.* **476**, 153–164 (2017).
9. Buczkowski, D. L. et al. The geomorphology of Ceres. *Science* **353**, aaf4332 (2016).
10. Park, R. S. et al. A partially differentiated interior for (1) Ceres deduced from its gravity field and shape. *Nature* **537**, 515–517 (2016).
11. Williams, D. A. et al. Introduction: the geologic mapping of Ceres. *Icarus* https://doi.org/10.1016/j.icarus.2017.05.004 (2018).
12. Greeley, R. & Spudis, P. D. Volcanism on Mars. *Rev. Geophys. Space Phys.* **19**, 13–41 (1981).
13. Stein, N. T. et al. The formation and evolution of bright spots on Ceres. *Icarus* https://doi.org/10.1016/j.icarus.2017.10.014 (2018).
14. Goldsby, D. L. & Kohlstedt, D. L. Superplastic deformation of ice: experimental observations. *J. Geophys. Res.* **106**, 11017–11030 (2001).
15. Durham, W. B., Pathare, A. V., Stern, L. A. & Lenferink, H. J. Mobility of icy sand packs, with application to Martian permafrost. *Geophys. Res. Lett.* **36**, L23203 (2009).
16. Bramson, A. M., Byrne, S. & Bapst, J. Preservation of midlatitude ice sheets on Mars. *J. Geophys. Res. Planets* **122**, 2250–2266 (2017).
17. Zambon, F. et al. Spectral analysis of Ahuna Mons from Dawn mission's visible-infrared spectrometer. *Geophys. Res. Lett.* **44**, 97–104 (2017).
18. Ruesch, O. et al. Geology of Ceres' north pole quadrangle with Dawn FC imaging data. *Icarus* https://doi.org/10.1016/j.icarus.2017.09.036 (2018).
19. Bland, M. T. et al. Why is Ceres lumpy? Surface deformation induced by solid-state subsurface flow. In *49th Lunar and Planetary Science Conference* 1627 (LPI, 2018).
20. Golombek, M. P. et al. Small crater modification on Meridiani Planum and implications for erosion rates and climate change on Mars. *J. Geophys. Res. Planets* **119**, 2522–2547 (2014).
21. Fassett, C. I. et al. Evidence for rapid topographic evolution and crater degradation on Mercury from simple crater morphometry. *Geophys. Res. Lett.* **44**, 5326–5335 (2017).
22. Platz, T. et al. Geological mapping of the Ac-10 Rongo quadrangle of Ceres. *Icarus* https://doi.org/10.1016/j.icarus.2017.08.001 (2018).
23. Marchi, S. et al. The missing large impact craters on Ceres. *Nat. Commun.* **7**, 12257 (2016).
24. De Sanctis, M. C. et al. Bright carbonate deposits as evidence of aqueous alteration on (1) Ceres. *Nature* **536**, 54–57 (2016).
25. Ruesch, O. et al. Bright carbonate surfaces on Ceres as remnants of salt-rich water fountains. *Icarus* https://doi.org/10.1016/j.icarus.2018.01.022 (2018).
26. Quick, L. C. et al. A possible brine reservoir beneath Occator crater: thermal and composition evolution and formation of the Cerealia dome and Vinalia Faculae. *Icarus* https://doi.org/10.1016/j.icarus.2018.07.016 (2018).
27. Nathues, A. et al. Evolution of Occator crater on (1)Ceres. *Astron. J.* **153**, 112 (2017).
28. Taisne, B. & Jaupart, C. Magma degassing and intermittent lava dome growth. *Geophys. Res. Lett.* **35**, L20310 (2008).
29. Sori, M. M., Zuber, M. T., Head, J. W. & Kiefer, W. S. Gravitational search for cryptovolcanism on the Moon: evidence for large volumes of early igneous activity. *Icarus* **273**, 284–295 (2016).
30. Crisp, J. A. Rates of magma emplacement and volcanic output. *J. Volcanol. Geotherm. Res.* **20**, 177–211 (1984).
31. Grimm, R. E. & Solomon, S. C. Limits on modes of lithospheric heat transport on Venus from impact crater density. *Geophys. Res. Lett.* **14**, 538–541 (1987).
32. Head, J. W. & Wilson, L. Lunar mare volcanism: stratigraphy, eruption conditions, and the evolution of secondary crusts. *Geochem. Cosmochim. Acta* **56**, 2155–2175 (1992).
33. Greeley, R. & Schneid, B. D. Magma generation on Mars: amounts, rates, and comparisons with Earth, Moon, and Venus. *Science* **254**, 996–998 (1991).
34. Zahnle, K., Alvarellos, J. A., Dobrovolskis, A. & Hamill, P. Secondary and sesquinary craters on Europa. *Icarus* **194**, 660–674 (2008).
35. Gross, P., van Wyk de Vries, B., Euillades, P. A., Kervyn, M. & Petrinovic, I. A. Systematic morphometric characterization of volcanic edifices using digital elevation models. *Geomorphology* **136**, 114–131 (2012).
36. Euillades, L. D., Grosse, P. & Euillades, P. A. NETVOLC: an algorithm for automatic delimitation of volcano edifice boundaries using DEMs. *Comput. Geosci.* **56**, 151–160 (2013).
37. Ermakov, A. I. et al. Constraints on Ceres' internal structure and evolution from its shape and gravity measured by the Dawn spacecraft. *J. Geophys. Res. Planets* **122**, 2267–2293 (2017).
38. Gagliardini, O. et al. Capabilities and performance of Elmer/Ice, a new-generation ice sheet model. *Geosci Model Dev.* **6**, 1299–1318 (2013).
39. Sori, M. M., Byrne, S., Hamilton, C. W. & Landis, M. E. Viscous flow rates of icy topography on the north polar layered deposits of Mars. *Geophys. Res. Lett.* **43**, 541–549 (2016).
40. McCarthy, C., Cooper, R. F., Goldsby, D. L., Durham, W. B. & Kirby, S. H. Transient and steady state creep response of ice I and magnesium sulfate hydrate eutectic aggregates. *J. Geophys. Res.* **116**, E04007 (2011).
41. Durham, W. B., Kirby, S. H. & Stern, L. A. Effects of dispersed particulates on the rheology of water ice at planetary conditions. *J. Geophys. Res.* **97**, 20833–20897 (1992).
42. Durham, W. B., Stern, L. A., Kubo, T. & Kirby, S. H. Flow strength of highly hydrated Mg- and Na-sulfate hydrate salts, pure and in mixtures with water ice, with application to Europa. *J. Geophys. Res.* **110**, E12010 (2005).
43. Wieczorek, M. A. et al. The crust of the Moon as seen by GRAIL. *Science* **339**, 671–675 (2013).
44. Soderblom, J. M. et al. The fractured Moon: production and saturation of porosity in the lunar highlands from impact cratering. *Geophys. Res. Lett.* **42**, 6939–6944 (2015).
45. Castillo-Rogez, J. C. et al. Ceres' geophysical evolution inferred from Dawn data. *AAS/Division for Planet. Sci.* **48**, 407.05 (2016).
46. Ermakov, A. I. et al. Ceres's obliquity history and its implications for the permanently shadowed regions. *Geophys. Res. Lett.* **44**, 2652–2661 (2017).

Acknowledgements

M.M.S., S.B., H.G.S. and M.T.B. acknowledge support from the National Aeronautics and Space Administration (NASA) Dawn Guest Investigator Program. Any use of trade, firm or product names is for descriptive purposes only and does not imply endorsement by the US Government.

Author contributions

M.M.S. formulated the project, performed all viscous flow model runs and led writing of this paper. M.M.S. and H.G.S. identified and analysed the domes suitable for this study. A.M.B. performed the thermal model runs. All authors contributed substantially to the interpretation of results and writing of this paper.

Competing interests

The authors declare no competing interests.

Additional information

Supplementary information is available for this paper at https://doi.org/10.1038/s41550-018-0574-1.

Reprints and permissions information is available at www.nature.com/reprints.

Correspondence and requests for materials should be addressed to M.M.S.

Publisher's note: Springer Nature remains neutral with regard to jurisdictional claims in published maps and institutional affiliations.